NMR solution structure of dsDNA containing a bicyclic D-*arabino*-configured nucleotide fixed in an O4'-*endo* sugar conformation †

Henning V. Tømmerholt, Nanna K. Christensen, Poul Nielsen, Jesper Wengel, Paul C. Stein, Jens Peter Jacobsen and Michael Petersen*

Nucleic Acid Center ‡, Department of Chemistry, University of Southern Denmark, DK-5230 Odense M, Denmark. E-mail: mip@chem.sdu.dk

[3.2.0]bcANA is a D-*arabino*-configured bicyclic nucleotide with a 2'-*O*,3'-*C*-methylene bridge. We here present the high-resolution NMR structure of a [3.2.0]bcANA modified dsDNA nonamer with one modified nucleotide incorporated. NOE restraints were obtained by analysis of NOESY cross peak intensities using a full relaxation matrix approach, and subsequently these restraints were incorporated into a simulated annealing scheme for the structure determination. In addition, the furanose ring puckers of the deoxyribose moieties were determined by analysis of COSY cross peaks. The modified duplex adopts a B-like geometry with Watson–Crick base pairing in all base pairs and all glycosidic angles in the *anti* range. The stacking arrangement of the nucleobases appears to be unperturbed relative to the normal B-like arrangement. The 2'-*O*,3'-*C*-methylene bridge of the modified nucleotide is located at the brim of the major groove where it fits well into the B-type duplex framework. The sugar pucker of the [3.2.0]bcANA nucleotide is O4'-*endo* and this sugar conformation causes a change in the δ backbone angle relative to the C2'-*endo* deoxyribose sugar pucker. This change is absorbed locally by slight changes in the ε and ζ angles of the modified nucleotide. Overall, the [3.2.0]bcANA modifications fits very well into a B-like duplex framework and only small and local perturbations are observed relative to the unmodified dsDNA of identical base sequence.

Introduction

In general, the conformation of the flexible furanose moiety determines the overall helical structure of dsDNA duplexes. Thus, the two low-energy deoxyribose conformations, C3'-*endo* and C2'-*endo*, yield two distinctly different duplex types. In A-form structures, the furanose assumes a C3'-*endo* (*N*-type) conformation, while in B-form structures a C2'-*endo* (*S*-type) conformation is taken.[1] The energy barrier to interconversion between these low energy states is rather low[2] (~2 kcal mol⁻¹) leading to the high plasticity of DNA. A number of factors influence the conformational A⇌B equilibrium in dsDNA, *e.g.* base sequence and environmental effects such as the relative humidity or ionic strength. When hybridised with RNA, DNA strands are found in neither A- nor B-form geometries but rather in intermediate states due to repuckering of the deoxyriboses.[3–5]

Steric and electronic effects, *e.g.* anomeric and gauche effects, determine the exact conformational equilibrium of deoxyriboses. Thus, substitution of the native deoxyribose ring can shift the conformational equilibrium. For example, a strongly electronegative substituent at the C2'-*ribo* position shifts the equilibrium towards *N*-type conformation as do exchanging the O3' by a less electronegative atom such as nitrogen as done in N3'→P5' phosphoramidates.[6] Electronegative substituents at the C2'-*arabino* position would be expected to shift the sugar equilibrium towards *S*-type conformation, however, it has been shown by X-ray crystallography and NMR spectroscopy that 2'-F-*arabino* modified deoxyriboses assume an O4'-*endo* conformation when incorporated into oligonucleotides, probably due to steric clashes between the 2'-fluorine and the aromatic nucleobase proton.[7,8]

The O4'-*endo* conformation is a high-energy conformation for native deoxyriboses, and as such it is probably only sparsely populated in dsDNA duplexes or DNA–RNA hybrids, although the exact conformation of the deoxyriboses in DNA–RNA hybrids is still a matter of debate.[8,9] The deoxyriboses may be in fast interconversion between *N*- and *S*-type sugar puckers or may be fixed in O4'-*endo* conformations. Nevertheless, the structure derived on the NMR time-scale will show an average geometry, which in the former case will resemble an O4'-*endo* sugar pucker. Thus, modified nucleic acids with a sugar conformation engineered into an O4'-*endo* conformation are potentially interesting as mimics of deoxyriboses in DNA–RNA hybrids.

In the context of antisense oligonucleotides (AOs), RNases H are enzymes of interest as they selectively cleave the RNA strand of DNA–RNA or potentially AO–RNA hybrids.[10] It is proposed that the ability of these enzymes to distinguish substrates from non-substrates (dsDNA and dsRNA) is owing to the difference in minor groove width, with the minor groove of DNA–RNA hybrids being intermediate to that of dsDNA and dsRNA duplexes.[11] This minor groove width peculiar for DNA–RNA hybrids arises structurally because the RNA strand possesses *N*-type sugar puckers while the DNA strand possesses sugar puckers of either mixtures of *N*- and *S*-type or fixed O4'-*endo* ones.

In recent years, a number of chemically conformationally restricted nucleotides have been synthesised.[12–14] In these type of compounds, the sugar conformation can be engineered by adding an extra ring to the sugar moiety, thus obtaining bicyclic sugars.[15] Prime interest of these restricted nucleotides has been given to LNA (Fig. 1), locked in a C3'-*endo* conformation.[12] LNA modified oligonucleotides have shown extremely high
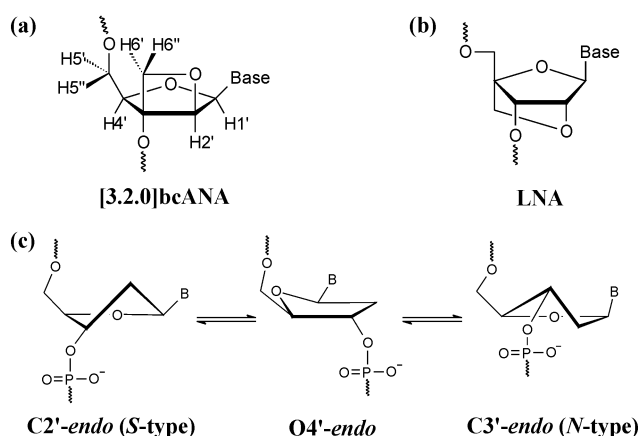
Fig. 1 (a) The chemical structure of a [3.2.0]bcANA nucleoside with the numbering of protons indicated. (b) The chemical structure of LNA. (c) The C2′-*endo*/C3′-*endo* interconversion passing through the O4′-*endo* conformation (the latter shown in a perpendicular view).

affinity towards cognate RNAs and DNAs, with increases in melting temperatures, ΔT_ms, ranging from $+3\,°C$ to $+10\,°C$ per LNA nucleotide incorporated.[12,16]

Recently, we have synthesised the 2′-*O*,3′-*C*-methylene linked D-*arabino*-configured bicyclic nucleoside [3.2.0]bcANA (Fig. 1).[17] By use of molecular modelling and NMR spectroscopy, we have shown that the furanose moiety adopts an O4′-*endo* conformation. That is, a conformation identical to that of 2′-F-ANA, however, the rationale for this sugar conformation is entirely different with the O4′-*endo* conformation of [3.2.0]-bcANA being due to the propensity of the fused oxetane ring to adopt an almost planar geometry.

The hybridization properties of [3.2.0]bcANA were evaluated, and in the context of DNA hybridization it was found that inclusion of up to four modifications in 9- or 14-mer oligonucleotides entailed almost unaltered melting temperatures, although four sequential modifications entailed a drop of ~1 °C per modification.[17] For a fully modified poly-T sequence, an increase in melting temperature of ~2 °C per modification was observed.

To assess the geometrical constraints of [3.2.0]bcANA when built into oligonucleotides, we have incorporated [3.2.0]bcANA once into a nonamer oligonucleotide (see Scheme 1). We have previously studied the unmodified version of this duplex and an LNA modified version,[18] thus we can compare the structure of the [3.2.0]bcANA modified duplex with these structures. By extracting vicinal proton coupling constants, we have determined the sugar conformations of the 17 deoxyriboses, and with the use of [1]H–[1]H NOEs, we have determined a high-resolution structure of the modified duplex.

$$\begin{array}{ccccccccc} 1 & 2 & 3 & 4 & 5 & 6 & 7 & 8 & 9 \end{array}$$
5′-d(C T G A T* A T G C)-3′
3′-d(G A C T A T A C G)-5′
$$\begin{array}{ccccccccc} 18 & 17 & 16 & 15 & 14 & 13 & 12 & 11 & 10 \end{array}$$
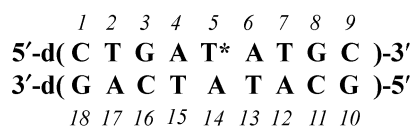
Scheme 1 The numbering scheme for the [3.2.0]bcANA:DNA duplex studied. T* denotes a [3.2.0]bcANA modified thymine monomer.

Results

Spectral analysis

The 1D ^{1}H NMR spectrum of the sample contains sharp lines from the expected dsDNA duplex (line widths ~3 Hz). The NOESY spectra of the duplex display the characteristic features of a right-handed double helix with all the nucleobases in the *anti* conformation. The assignment of proton resonances in the duplex was performed by standard methods.[19–22] The NOESY spectra with short mixing times allowed unambiguous

assignment of all H2′ and H2″ resonances and the H6′ and H6″ resonances in the modified nucleotide, T*5. The latter resonance pair was stereospecifically assigned by the magnitude of their NOESY cross peaks to the nucleobase proton of T*5. The chemical shift values and the NOE connectivity pattern of the imino protons are in accordance with normal Watson–Crick base pairing, thus justifying the inclusion of Watson–Crick restraints in the structure calculations. Chemical shifts are tabulated in the Electronic supplementary information† (Table S2).

The chemical shifts of the modified duplex and the corresponding unmodified dsDNA duplex are in close agreement. Aside from the central three base pairs, no difference in excess of 0.03 ppm is observed. In the modified nucleotide, H2′ has an upfield shift of 2.96 ppm compared with unmodified dsDNA owing to the introduction of an electronegative oxygen at C2′. Apart from this resonance, no shift of more than ~0.3 ppm is observed in the central three base pairs, this indicates a close structural resemblance between the modified and native duplexes. The largest change in chemical shift is observed for A4 H2″ ($\Delta\delta = 0.31$ ppm). Owing to the O4′-*endo* conformation of T*5, this proton is located fairly close to T*5 O4′, the distance being ~3.3 Å as compared with ~4.2 Å for nucleotides in *S*-type conformations.

Analysis of COSY spectra

For *S*-type deoxyriboses, large coupling constants are expected for H1′–H2″ and smaller coupling constants for H1′–H2′ and *vice versa* for *N*-type deoxyriboses. Consequently, the H1′–H2″ DQF-COSY cross peak of an *S*-type sugar has a fine structure which splits the peak into 16 components, whilst the H1′–H2′ cross peak has a much simpler fine structure. In contrast, for an *N*-type sugar, the H1′–H2″ cross peak has a simple fine structure, whilst the H1′–H2′ cross peak is either of low intensity or absent due to cancellation of antiphase peaks.

Qualitatively, the H1′ to H2′ and H2″ DQF-COSY cross peaks of the [3.2.0]bcANA modified duplex have the appearances of predominantly *S*-type deoxyribose conformations (see Fig. 2). The coupling constants of the sugar protons were obtained by analysis of the DQF-COSY spectrum and are given in Table 1. The DQF-COSY spectrum back calculated with these coupling constants resembles the experimental spectrum very well as shown in Fig. 2. Subsequently, the deoxyribose conformations were analysed assuming a two-state $N \rightleftharpoons S$ equilibrium and the fraction of *S*-type sugar conformations as well as the pseudorotation angles obtained are included in Table 1. Overall, fairly uniform deoxyribose conformations are observed along the duplex, with all deoxyribose sugars possessing in excess of 85% *S*-type conformation. These results are in agreement with those obtained for the unmodified duplex of identical base sequences as all deoxyribose sugars in this duplex also have predominant *S*-type sugar puckers.[18]

The modified nucleotide

As for the modified [3.2.0]bcANA sugar, unfortunately complete resonance degeneracy between the H1′ and H2′ protons precluded determination of the $J_{H1'H2'}$ coupling constant in the duplex sample. At the monomer level, a geometry optimisation of the [3.2.0]bcANA nucleoside carried out at the HF/6-31G* level yielded an O4′-*endo* sugar conformation ($P = 90°$, $\Phi_{max} = 38°$). This geometry gives a H1′H2′ torsion angle of 44.4°, which in turn yields $J_{H1'H2'} = 2.5$ Hz using a state-of-the-art Karplus relationship.[23–25] This coupling constant is in accordance with the experimental one,[17] thus validating the O4′-*endo* sugar pucker of the modified nucleoside.

Duplex structure calculations

A total of 40 structures were calculated for the [3.2.0]bcANA modified duplex employing a simulated annealing protocol as
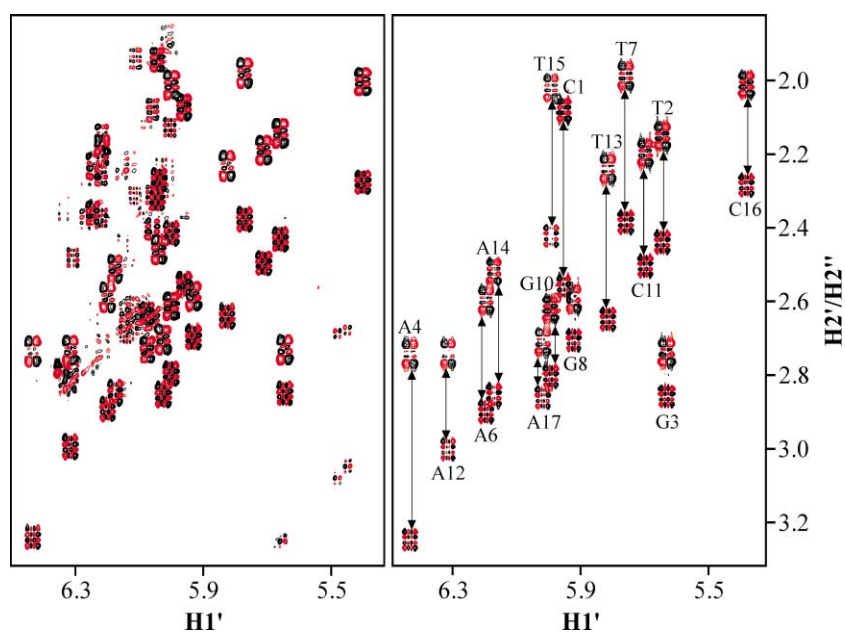
Fig. 2 Comparison of the H1′ to H2′/H2″ regions of the experimental (left) and the calculated (right) DQF-COSY spectra for the [3.2.0]bcANA modified duplex. In the calculated spectrum, the 15 cross peak pairs simulated are indicated. Weak cross peaks in the experimental spectrum are from traces of single-stranded species.

Table 1 Coupling constants for the sugar protons in the d(CTGA-T*ATGC)–d(GCATATCAG) duplex and the sugar conformations derived [a]

	$J_{1'2'}$/Hz	$J_{1'2''}$/Hz	$J_{2'3'}$/Hz	$J_{2''3'}$/Hz	%S [d]	$PSI/°$ [e]
C1	6.4	6.9	0.6	1.1	91 (7)	197 (9)
T2	9.2	5.8	3.8	0.9	95 (6)	174 (15)
G3	10.0	5.5	4.1	0.8	97 (6)	169 (10)
A4	9.8	5.2	4.8	1.2	95 (6)	162 (10)
T*5 [b]						
A6	8.9	5.7	4.4	2.2	86 (8)	167 (14)
T7	9.0	5.9	3.9	1.2	93 (8)	177 (15)
G8	8.7	5.5	4.7	1.0	91 (9)	167 (23)
C9 [c]						
G10	8.7	5.6	1.1	1.0	97 (5)	181 (8)
C11	8.9	5.3	3.9	0.9	95 (6)	175 (9)
A12	8.9	5.4	5.6	1.3	87 (9)	161 (18)
T13	9.4	5.7	5.1	1.8	89 (9)	164 (14)
A14	7.3	6.3	4.7	1.2	85 (12)	189 (17)
T15	8.1	5.6	4.2	1.1	90 (9)	181 (12)
C16	8.3	5.5	3.2	0.9	93 (8)	179 (15)
A17	8.4	5.8	4.8	0.9	91 (10)	177 (18)
G18 [c]						

[a] The coupling constants were derived from the H1′–H2′ and H1′–H2″ cross peaks in the selective DQF-COSY spectrum using CHEOPS. The $J_{2'2''}$ coupling constants returned were between −14.2 and −15.0 Hz, values typical for deoxyribose. The sugar conformations were calculated using a randomised version of the PSEUROT program. In PSEUROT calculations, the puckering amplitudes were fixed at 35°. The standard deviations are given in brackets. [b] The [3.2.0]bcANA nucleotide was not included in the CHEOPS calculations due to the restricted conformation. [c] No coupling constants were obtained for C9 and G18 due to spectral overlap. [d] Percent S-type sugar conformation calculated using PSEUROT. [e] Pseudorotation angle calculated for the S-type sugar conformation.

described in the Experimental section. Twenty random sets of initial velocities for each of the two starting structures (A- and B-type geometries) were used. All structures converged to one family of structures, with an all-atom RMSD of 1.11 Å for all base pairs and 0.91 Å for non-terminal base pairs (see Fig. 3). The final ensemble of structures features low distance restraint energies and low distance violations compared with the starting structures (see Table 2). The average sum of violations for the 40 structures is 5.85 Å and no violations larger than 0.22 Å were observed in any of the calculated structures.
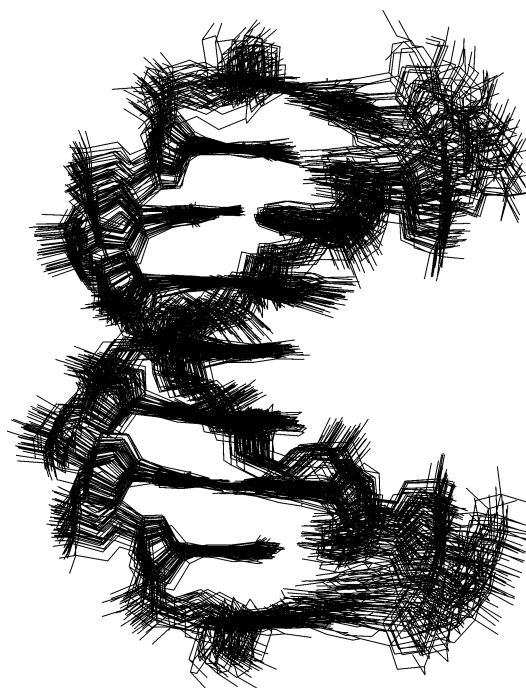
Fig. 3 A superposition of the 40 structures calculated for the [3.2.0]bcANA modified duplex from either A-type or B-type starting geometries. For clarity, hydrogen atoms are not shown.

General description of the structure

The calculated family of structures is in the domain of B-type helices as demonstrated by RMSD values of 1.8 Å between the calculated structure and the energy minimised B-form starting structure and 1.5 Å between the structure and the structure of the unmodified dsDNA.[18] In the structure, all glycosidic angles are in the *anti* conformation and Watson–Crick base pairing is maintained for all base pairs. The duplex is regular as shown by the nearly straight helix axis as calculated by CURVES5.2.[26,27] The helix axis pierces the nucleobases as is common for duplexes in the B-type domain. Other indications of the B-like appearance of the structure are the narrow and deep minor groove (average width ~6.1 Å) and intra-strand phosphorous distances of ~7 Å. A stereo view of the duplex is shown in Fig. 4.

Table 2 Structural parameters for the NOE derived structure[a]

Structure	E_{AMBER}/kcal mol^{-1}	E_{NOE}/kcal mol^{-1}	Δd_{av}/Å	RMSD *vs* NMR/Å
A-type	−21.5	5042	0.481	3.00 (0.44)
B-type	−48.1	818.4	0.111	1.83 (0.47)
NMR	−0.5	24.2	0.018	0.91 (0.41)[b]

[a] Force field (E_{AMBER}) and restraint (E_{NOE}) energies, average restraint violations (Δd_{av}) and pairwise atomic RMSDs for the starting structures and the NMR structure. All-atomic RMSDs were calculated for all atoms of the seven internal base pairs. Where applicable, standard deviations are included in brackets. [b] Atomic RMSDs for the 40 structures calculated from A-form and B-form starting geometries.
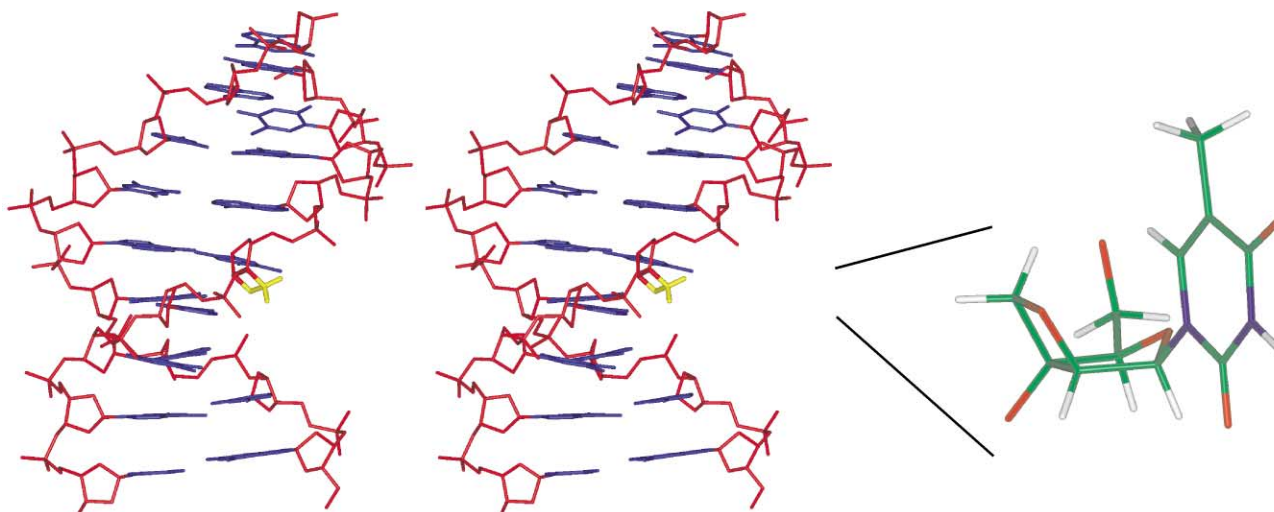
Fig. 4 Stereo view of the structure of the [3.2.0]bcANA modified duplex (left). For clarity, only hydrogens on the modification are shown. The colouring scheme is: The nucleobases, blue; the sugar–phosphate backbone, red; and the [3.2.0]bcANA 2′-*O*,3′-*C* bridge, yellow. Detailed view of T*5 showing the O4′-endo sugar conformation (right). The atoms are coloured individually.

The B-like appearance of the [3.2.0]bcANA modified duplex is corroborated by its CD spectrum (included in the Electronic supplementary information†). This spectrum displays the characteristics of B-type duplex geometries, *i.e.* no negative band at ~210 nm, a negative band at ~250 nm and a positive one at ~270 nm, these two bands having approximately equal magnitude.

In the structure, the modified [3.2.0]bcANA nucleotide adopts an O4′-*endo* sugar conformation ($P = 86°$, $\Phi_{max} = 34°$), and the 2′-*O*,3′-*C*-methylene bridge of T*5 is located at the brim of the major groove (see Fig. 4). There it fits snugly in a pocket created by one of the non-bridging phosphate oxygens of A6, O5′ of T5, and the nucleobase protons of T5 and A6, with the oxymethylene bridge being in van der Waals contacts with these atoms.

The nucleobase of T*5 stacks with A4's nucleobase while there is no overlap with the base of A6. This stacking arrangement is perfectly similar to what is usually observed for B-type duplexes and is also what is observed for other ApT and TpA base steps in this duplex. In accordance with other B-type duplex structures, we observe no inter-strand stacking.

Helix parameters

Helix parameters and the global helix axis were calculated using CURVES5.2 (a table with a selection of helical parameters is included in the Electronic supplementary information†; Table S3). The global helix axis is fairly straight with a slight bend at the T2pG3–C16pA17 base pair step (~11°), this shows that the single [3.2.0]bcANA nucleotide is incorporated into the dsDNA duplex without introducing global incoherences. X-displacement, Y-displacement, inclination, and tip are the helix parameters with which the global helix axis is determined. Consequently, these parameters allow a direct comparison between A- and B-type duplex forms and the structure determined. The values for X-displacement and inclination are near the values expected for a B-type duplex. Y-displacement and tip offer no

discrimination between different duplex forms, however, these parameters serve as to describe the regularity of the duplex, with only slight variations along the duplex (up to 0.3 Å for Y-displacement and 9.2° for tip). As for the remaining helix parameters, most only show fairly slight variations along the duplex, however, with the T2pG3–C16pA17 base pair step displaying a number of extreme values, *e.g.* roll of 11°, buckle of 20°, tilt of −8° and opening of −6°. Large values for roll, indicating bending of the helix axis, are usual for TpG–CpA base pair steps[28] and the negative value of opening shows that the bend is towards the major groove. Propeller twist is negative for all base pairs except for C1–G18, with an average value of −9.5°. The average value for rise is 3.1 Å which is close to the value for a standard B-type duplex (3.4 Å), a slightly lower value for rise (2.8 Å) is observed in the T*5pA6–T13pA14 step. For twist, the average value is 32.8°, which is a slight unwinding relative to standard B-DNA, however, slight unwinding appears to be common for many NMR derived structures.[29]

Backbone geometry

Due to the intrinsic paucity of NOE restraints in the DNA phosphate backbone, the backbone geometry of the duplex is less precisely determined than the geometry of the nucleobases in the structure. Rather, the backbone geometry is determined by the force field employed and by the constraints imposed by the placement of the nucleobases, for stacking and base pairing, and the sugars. Most of the sugar–phosphate backbone torsion angles reside in the domains of the standard genus for B-type DNA duplexes. A few exceptions are observed in the unmodified DNA strand, with two *a*-angles residing in the gauche+ range (T13 and A17) and two *γ*-angles in the *trans* domain (C11 and T13), these deviations from standard values are a consequence of the malleability of the DNA backbone as encoded in the force field of Cornell *et al.*[30] As for the modified [3.2.0]bcANA nucleotide, the change in the *δ*-angle brought about by the locked O4′-*endo* sugar conformation is counter-

Table 3 Backbone torsion angles for the [3.2.0]bcANA modified nucleotide (T*5) and its neighbouring nucleotides, together with the glycosidic angles, pseudorotation angles and puckering amplitudes (all in degrees)

Residue	α	β	γ	δ	ε	ζ	χ	P	Φ_{max}
A4	−69	−139	43	148	180	−91	−100	181	35
T*5	−75	−191	65	85	164	−66	−136	86	34
A6	−56	−179	45	126	178	−95	−120	140	32

acted by slight changes in the ε- and ζ-angles (see Table 3). The glycosidic angles, χ, are found in *anti* conformations for all nucleotides as was expected by inspection of the NOESY spectra. For the modified nucleotide, we find a glycosidic angle of −136°. This magnitude of the glycosidic angle appears to be favourable for positioning the nucleobase in a geometry suitable for Watson–Crick base pairing for nucleotides with O4′-*endo* sugar puckers.[7,8,31] For the unmodified nucleotides, the average glycosidic angle is −117°, close to the standard B-type value of −108°.

Sugar conformations

All deoxyribose sugars in the structure have *S*-type conformations, with pseudorotation angles between $P = 112°$ (C16) and $P = 194°$ (T13) for non-terminal residues and an average pseudorotation angle of $P = 149°$. These sugar conformations are in general agreement with the results obtained by analysis of the sugar coupling constants (see above). The pseudorotation angle of the modified [3.2.0]bcANA nucleotide is 86° and the puckering amplitude 34°. These values are in good agreement with the values determined by *ab initio* calculations, thus validating the force field employed in the structure calculations as suitable in reproducing the geometry of the [3.2.0]bcANA nucleotide.

Discussion

The [3.2.0]bcANA modified duplex exhibits NMR spectral features typical of a right-handed DNA helix possessing an overall B-like geometry with all nucleobases in *anti* conformations and forming normal Watson–Crick base pairing. Comparing the chemical shifts of this modified duplex with the corresponding unmodified one,[18] we observe only the slightest of changes (less than 0.03 ppm) except for the A4pT*5pA6-fragment, where shifts of up to ~0.3 ppm are observed (H2′ of T*5 obviously has a large upfield change owing to the electronegative O2′ atom introduced). This invariance in chemical shifts demonstrates that only local and slight structural changes are taking place upon incorporation of the [3.2.0]bcANA nucleotide. Particularly, the chemical shift invariance of the adenines' H2 protons is notable. With the H2 proton of adenines being sited near the centre of the duplex, chemical shift changes of these protons are indicators of changes in base stacking. Thus, it appears that, probably, no major changes in nucleobase stacking are occurring upon modification of the T5 nucleotide. This is consistent with the B-like stacking arrangement we observe.

The structural similarity between the [3.2.0]bcANA modified duplex and the corresponding unmodified duplex is also demonstrated by CD spectroscopy with the spectra of the two duplexes being virtually undistinguishable. Likewise, the modified and unmodified duplexes have identical melting temperatures.[32]

Our analyses of the deoxyribose sugar conformations in the [3.2.0]bcANA modified duplex show that all deoxyribo sugars adopt almost pure *S*-type sugar puckers. This is consistent with the B-like appearance as indicated by analyses of NOESY spectra.

In this context, the high-resolution structure of the [3.2.0]-bcANA modified duplex possesses the general appearance of

a B-type duplex as indicated by the base planes being nearly perpendicular to the helix axis, by a number of helical parameters as described above, and by sugar conformations in the *S*-type range of the pseudorotation cycle. In addition, we find an average minor groove width of 6.1 Å, which is near the value expected for a B-type duplex. In the corresponding unmodified dsDNA duplex, an identical minor groove width was observed.[18] Thus, the incorporation of the [3.2.0]bcANA nucleotide appears to leave the structure of the duplex strikingly unperturbed relative to the unmodified dsDNA as is also shown by the B-like sugar–phosphate backbone.

The [3.2.0]bcANA modified nucleotide adopts an O4′-*endo* furanose conformation in the NMR structure. This conformation is determined mutually by the force field applied in the calculations and by the NMR derived distance restraints, and is in good agreement with the conformation of the modified nucleoside as calculated by *ab initio* methods. The fixed sugar conformation of the modified nucleotide imposes a change of ~50° for the δ-angle of T*5, this change is absorbed by the DNA backbone by slight changes in the ε- and ζ-angles of T*5. This is identical to what is also observed for other modified nucleotides adopting O4′-*endo* conformations.[7,8]

The 2′-O,3′-C-methylene bridge of the modified nucleotide is located at the brim of the major groove, where it sterically fits well between its own nucleobase and the 3′-flanking one (see Fig. 4). Even though the oxymethylene bridge makes van der Waals contacts with neighbouring nucleotides, it appears to leave both the nucleobase stacking arrangement and the sugar–phosphate backbone unaltered relative to normal B-DNA.

The O4′-*endo* sugar conformation is interesting in as much as it is a high-energy conformation in the pseudorotational pathway for deoxyriboses, defining the energy barrier to interconversion between C2′-*endo* and C3′-*endo* conformations (see Fig. 1).[2] In DNA–RNA hybrids, the deoxyribo nucleotides are repuckering between C2′-*endo* and C3′-*endo* sugar conformations, and from structural studies, it appears that the O4′-*endo* conformation is a good mimic of the average deoxyribose sugar pucker in this case.[31,33]

Some other modified nucleic acids possess O4′-*endo* puckers, *e.g.* 2′-F-ANA and [3.3.0]bcANA, a close analogue of [3.2.0]bcANA with a 2′-O,3′-C-ethylene bridge. Both of these nucleotide analogues were incorporated into dsDNA duplexes and studied by X-ray crystallography and NMR spectroscopy.[7,8,31] In common for these structures is that the modified nucleotides only perturb the duplex structure locally and only slightly. That is the duplexes retain an overall B-like appearance. As for our [3.2.0]bcANA NMR structure, the changes in the δ backbone torsion angle brought about by the O4′-*endo* sugar conformation of the modified nucleotides are absorbed by the DNA phosphate backbone by changes in the ε and ζ-torsion angles of the modified nucleotides. This demonstrates the high malleability of the DNA phosphate backbone and its unique capability to absorb perturbations with only minimal distortion of the global duplex structure resulting.

LNA is a nucleotide analogue locked in a C3′-*endo* (*N*-type) sugar conformation. We have previously studied a number of LNA modified dsDNA duplexes and have found that LNA nucleotides perturb the duplex structure towards an A-type

geometry. Thus the incorporation of LNA nucleotides in dsDNA entail more dramatic structural changes than does the incorporation of [3.2.0]bcANA nucleotides. In particular, in a dsDNA duplex with one LNA nucleotide incorporated, we found that the nucleotide 3′-flanking the LNA nucleotide possessed ~40% N-type sugar conformation,[34] no such perturbation of neighbouring nucleotides is observed in the [3.2.0]bcANA modified dsDNA duplex. The 86 ± 8% S-type sugar conformation found for A6 in this work is well in line with the amount of S-type conformation determined for unmodified dsDNA duplexes. In X-ray crystallographic structures, the incorporation of O4′-endo modified analogues (2′-F-ANA or [3.3.0]bcANA) leaves the bulk of the dsDNA unperturbed, that is the overall duplex geometry is B-like,[7,31] however, incorporation of two LNA nucleotides in a dsDNA duplex propels the entire duplex into an A-type geometry with all deoxyriboses having N-type sugar puckers,[35] i.e. a more dramatic effect than in solution. Similarly, incorporation of two terminal RNA nucleotides in dsDNA alter the entire duplex geometry to A-type with the deoxyriboses having N-type sugar puckers as determined by X-ray crystallography.[36] As both ribonucleotides and LNA nucleotides contain a 2′-ribo oxygen (and [3.2.0]bcANA does not), this may be the key factor triggering the crystallisation in A-type of RNA and LNA modified dsDNAs; an alternative possibility is that a single nucleobase positioned in an A-like stacking arrangement can trigger a conformational B to A shift throughout a duplex in order to maximise stacking interactions. However, the observation that O4′-endo fixed nucleotides cannot induce a B to A shift shows that it is fairly subtle structural changes and energetics that trigger such a conformational shift.

In a biological context, DNA–RNA hybrids are interesting as RNase H cleaves the RNA strand of such hybrids. In the antisense approach, one of the possible mechanisms is that the antisense oligonucleotide (AO) binds to the cognate mRNA and the AO–mRNA hybrid is recognised by RNase H with subsequent cleavage and silencing of the mRNA. As the O4′-endo sugar pucker appears to be a mimic of a repuckering deoxyribose, nucleic acid analogues engineered to possess this sugar conformation are structurally interesting in the context of RNase H recognition. 2′-F-ANA–RNA hybrids act as substrates for RNase H with subsequent scission of the RNA strand.[37] In a homo-thymine–homo-adenylate 14-mer duplex context, a [3.2.0]bcANA–RNA hybrid did not elicit RNase H activity, nor did the corresponding [3.3.0]bcANA–RNA hybrid.[38] Structural studies have shown that the latter analogue also possesses an O4′-endo sugar conformation.[31,39] This indicates that factors beside sugar conformations are important for RNase H recognition. This could for example be a steric interaction between the 2′-O,3′-C-bridge and the enzyme or that slight changes in the sugar–phosphate backbone of the modified strand alter the interactions between the hybrid and the primer grip of RNase H[40] and hence positions potentially scissile RNA phosphates in non-optimum geometries for cleavage. Moreover, it should be noted that no general conclusions on the RNase H substrate properties of bcANAs can be drawn as so far as only the rather unusual homo-thymine sequence has been studied.

In conclusion, we have determined the structure of a nonamer dsDNA duplex with a single [3.2.0]bcANA modification incorporated. Altogether the O4′-endo conformation of the [3.2.0]bcANA modified nucleotide (T*5) is compatible with the B-form duplex geometry of dsDNA and consequently, the overall duplex geometry is B-type. The additional 2′-O,3′-C-methylene bridge of T*5 fits snugly into the B-form framework of the duplex and the modified nucleotide is well accommodated in the duplex. The small changes imposed in the sugar–phosphate backbone due to the O4′-endo sugar pucker of T*5 are absorbed locally by changes in the ε and ζ-angles of T*5.

Experimental

Sample preparation

The d(CTGAT*ATGC) oligonucleotide was synthesised as described elsewhere.[17] The unmodified complementary oligonucleotide was purchased from DNA Technology, Århus, Denmark. Both oligonucleotides were purified by site-exclusion on a Sephadex G15 column. The duplex was obtained by dissolving equimolar amounts of the complementary strands in 0.5 mL of 10 mM sodium phosphate buffer (pH 7.0), 0.05 mM NaEDTA and 0.01 mM NaN_3. The numbering scheme used for the duplex is shown in Scheme 1.

For experiments carried out in D_2O the solid duplex was lyophilised three times from D_2O and redissolved in 99.96% D_2O (Cambridge Isotope Laboratories). A mixture of 90% H_2O and 10% D_2O (0.5 mL) was used for experiments examining exchangeable protons. The final concentration of the duplex was 2 mM.

NMR experiments

NMR experiments were performed on either a Varian UNITY 500 or a Varian INOVA 800 spectrometer at 25 °C. NOESY spectra with mixing times of 50, 100, 150 and 200 ms were acquired sequentially without removing the sample from the magnet at 800 MHz in D_2O using 2048 complex points in t_2 and a spectral width of 8000 Hz. A total of 800 t_1 experiments, each with 32 scans and a dwell-time of 4.8 s between scans, were recorded using the States phase cycling scheme. The residual signal from HOD was removed by low-power presaturation. Furthermore, an inversion recovery experiment was performed at 800 MHz. A NOESY spectrum in H_2O was acquired at 800 MHz using the WATERGATE pulse sequence with spectral widths of 16000 Hz using 2048 complex points, 512 t_1 experiments, each with 48 scans. A TOCSY spectrum with a mixing time of 90 ms was obtained at 500 MHz. In addition, a selective DQF-COSY spectrum was acquired at 500 MHz using a pulse sequence in which the first pulse was replaced with an E-BURP type selective pulse[41] in order to enhance the digital resolution in F1. This spectrum was acquired with spectral widths of 5000 Hz in F2 and 1200 Hz in F1, respectively, and a total of 720 t_1 experiments, each with 64 scans, with 2048 complex points in t_2.

The acquired data were processed using FELIX (version 98, MSI, San Diego, CA). All spectra were apodised by skewed sinebell squared functions in F1 and F2 and baseline corrected using the FLATT algorithm in F2 and the automatic baseline flattening algorithm in F1.

The H1′ to H2′ and H2″ regions of the DQF-COSY spectra were used as input to CHEOPS to obtain J coupling constants for the H1′, H2′, H2″, and H3′ deoxyribose ring protons.[42] The deoxyribose conformations were derived by use of PSEUROT[43] assuming a fast two-state equilibrium between two conformations (N- and S-type) in a manner as previously described.[44]

Distance restraints

The upper and lower parts of each of the NOESY build up spectra were integrated separately with FELIX, yielding eight peak intensity sets. The integrated peak intensities were corrected for saturation effects using the T_1 relaxation times obtained from the inversion recovery experiment. The RANDMARDI procedure[45] of the complete relaxation matrix analysis method MARDIGRAS[46] was used to calculate the interproton distances from the peak intensity sets. In the calculations, an absolute noise level of the same order of magnitude as the smallest integrated cross peak was used. A relative integration error for each peak was set at 10% of the integrated peak intensity throughout the calculations. In the calculations, an isotropic correlation time of 2.0 ns was applied. In the RANDMARDI procedure, 30 different intensity sets were

generated from each experimental data set based on the given noise level and integration error, and MARDIGRAS calculations were performed on all of them. The distances resulting from all generated intensity sets were combined into a single distance bound file by averaging the distances returned for each peak intensity set, with the upper and lower bounds, respectively, being the average distance ± one standard deviation. Prior to inclusion in calculations, an additional 0.3 Å was added to all upper bounds. After this, the average flat well width obtained was 0.72 Å. The procedure described resulted in a total of 291 distance restraints for inclusion in the structure determination. A break down of these restraints is shown in Fig. 5. In addition to the restraints described above, 22 restraints mimicking Watson–Crick base pairing were included. Target values for these restraints were taken from crystallographic data.[1] No restraints were included to restrain the sugar–phosphate backbone.
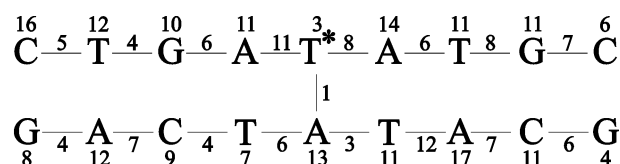
Fig. 5 The distribution of the NOE restraints obtained from RANDMARDI calculations. The numbers of intra-nucleotide, sequential and cross-strand restraints are indicated.

Structure calculations

All calculations were performed with the AMBER5 suite of programs[47] on SGI/O2 workstations employing the force field of Cornell et al.[30] A simulated annealing procedure was utilised to obtain the NMR structure of the [3.2.0]bcANA modified duplex. Two different starting structures (A- and B-form duplexes), obtained with the *nucgen* module of AMBER5, were used. The appropriate nucleotide was modified to a [3.2.0]bcANA nucleotide and atomic charges for the modified nucleotide were calculated using the RESP procedure (A Table showing atomic charges for the thymidine [3.2.0]bcANA nucleoside is included in the Electronic supplementary information†).[48]

Each structure was initially restrained energy minimised before being subjected to 28 ps of molecular dynamics in time-steps of 1 fs: 5 ps at 800 K followed by cooling to 300 K over 23 ps, over the first picosecond of simulation, the NOE force constants were ramped up from 5 kcal mol^{-1} Å^{-2} to 200 kcal mol^{-1} Å^{-2}, held at this value for 4 ps and gradually lowered to 50 kcal mol^{-1} Å^{-2} during the remaining 23 ps of simulation. Finally, a further restrained energy minimisation was carried out. A distance dependent dielectric constant, $\varepsilon = 4r$, was used and the non-bonded cut-off was 16 Å.

References

1 W. Saenger, *Principles of Nucleic Acid Structure*, Springer Verlag, New York, 1984.
2 K. A. Brameld and W. A. Goddard III, *J. Am. Chem. Soc.*, 1999, **121**, 985.
3 C. Gonzáles, W. Stec, M. Reynolds and T. L. James, *Biochemistry*, 1995, **34**, 4969.
4 T. E. Cheatham III and P. A. Kollman, *J. Am. Chem. Soc.*, 1997, **119**, 4805.
5 J. I. Gyi, A. N. Lane, G. L. Conn and T. Brown, *Biochemistry*, 1998, **37**, 73.
6 S. M. Gryaznov, *Biochim. Biophys. Acta*, 1999, **1489**, 131.
7 I. Berger, V. Tereshko, H. Ikeda, V. E. Marquez and M. Egli, *Nucleic Acids Res.*, 1998, **26**, 2473.
8 J.-F. Trempe, C. J. Wilds, A. Y. Denisov, R. T. Pon, M. J. Damha and K. Gehring, *J. Am. Chem. Soc.*, 2001, **123**, 4896.
9 A. Y. Denisov, A. M. Noronha, C. J. Wilds, J.-F. Trempe, R. T. Pon, K. Gehring and M. J. Damha, *Nucleic Acids Res.*, 2001, **29**, 4284.
10 J.-J. Toulmé and D. Tidd, Role of Ribonuclease H in Antisense Oligonucleotide-Mediated Effects, in *Ribonucleases H*, ed. R. J. Crouch and J.-J. Toulmé, INSERM, Paris, 1998, 225.
11 O. Y. Fedoroff, M. Salazar and B. R. Reid, *J. Mol. Biol.*, 1993, **233**, 509.
12 J. Wengel, *Acc. Chem. Res.*, 1999, **32**, 301.
13 P. Herdewijn, *Biochim. Biophys. Acta*, 1999, **1489**, 167.
14 C. J. Leumann, *Bioorg. Med. Chem.*, 2002, **10**, 841.
15 M. Meldgaard and J. Wengel, *J. Chem. Soc., Perkin Trans 1*, 2000, 3539.
16 D. A. Braasch and D. R. Corey, *Chem. Biol.*, 2001, **8**, 1.
17 N. K. Christensen, M. Petersen, P. Nielsen, J. P. Jacobsen, C. E. Olsen and J. Wengel, *J. Am. Chem. Soc.*, 1998, **120**, 5458.
18 G. A. Jensen, S. K. Singh, R. Kumar, J. Wengel and J. P. Jacobsen, *J. Chem. Soc., Perkin Trans. 2*, 2001, 1224.
19 D. R. Hare, D. E. Wemmer, S.-H. Chou, G. Drobny and B. R. Reid, *J. Mol. Biol.*, 1983, **171**, 319.
20 J. Feigon, W. Leupin, W. A. Denny and D. R. Kearns, *Biochemistry*, 1983, **22**, 5943.
21 R. M. Scheek, N. Russo, R. Boelens and R. Kaptein, *J. Am. Chem. Soc.*, 1983, **105**, 2914.
22 K. Wüthrich, *NMR of Proteins and Nucleic Acids*, John Wiley & Sons, New York, 1986.
23 L. A. Donders, F. A. A. M. de Leeuw and C. Altona, *Magn. Reson. Chem.*, 1989, **27**, 556.
24 C. Altona, J. H. Ippel, A. J. A. Westra Hoekzema, C. Erkelens, M. Groesbeek and L. A. Donders, *Magn. Reson. Chem.*, 1989, **27**, 564.
25 C. Altona, R. Francke, R. de Haan, J. H. Ippel, G. J. Daalmans, A. J. A. Westra Hoekzema and J. van Wijk, *Magn. Reson. Chem.*, 1994, **32**, 670.
26 R. Lavery and H. Sklenar, *J. Biomol. Struct. Dyn.*, 1988, **6**, 63.
27 R. Lavery and H. Sklenar, *J. Biomol. Struct. Dyn.*, 1989, **7**, 655.
28 N. A. Ulyanov and T. L. James, *Methods Enzymol.*, 1995, **261**, 90.
29 C. H. Gotfredsen, H. P. Spielmann, J. Wengel and J. P. Jacobsen, *Bioconjugate Chem.*, 1996, **7**, 680.
30 W. D. Cornell, P. Cieplak, I. Bayly, I. R. Gould, K. M. Merz, D. M. Ferguson, D. C. Spellmeyer, T. Fox, J. W. Caldwell and P. A. Kollman, *J. Am. Chem. Soc.*, 1995, **117**, 5179.
31 G. Minasov, M. Teplova, P. Nielsen, J. Wengel and M. Egli, *Biochemistry*, 2000, **39**, 3525.
32 The melting temperature of the [3.2.0]bcANA modified duplex was measured under conditions as described by Christensen *et al.* (ref. 17).
33 M. Petersen, K. Bondensgaard, J. Wengel and J. P. Jacobsen, *J. Am. Chem. Soc.*, 2002, **124**, 5974.
34 C. B. Nielsen, S. K. Singh, J. Wengel and J. P. Jacobsen, *J. Biomol. Struct. Dyn.*, 1999, **17**, 175.
35 M. Egli, G. Minasov, M. Teplova, R. Kumar and J. Wengel, *Chem. Commun.*, 2001, 651.
36 M. Egli, N. Usman and A. Rich, *Biochemistry*, 1993, **32**, 3221.
37 M. J. Damha, C. J. Wilds, A. Noronha, I. Brukner, G. Borkow, D. Arion and M. A. Parniak, *J. Am. Chem. Soc.*, 1998, **120**, 12976.
38 H. Brummel, N. K. Christensen and M. H. Caruthers, Personal communication.
39 L. B. Jørgensen, P. Nielsen, J. Wengel and J. P. Jacobsen, *J. Biomol. Struct. Dyn.*, 2000, **18**, 45.
40 S. G. Sarafianos, K. Das, C. Tantillo, A. D. Jr. Clark, J. Ding, J. M. Whitcomb, P. L. Boyer, S. H. Hughes and E. Arnold, *EMBO J.*, 2001, **20**, 1449.
41 H. Geen and R. Freeman, *J. Magn. Reson.*, 1991, **93**, 93.
42 R. F. Macaya, P. Schultze and J. Feigon, *J. Am. Chem. Soc.*, 1992, **114**, 781.
43 C. A. G. Haasnoot, F. A. A. M. de Leeuw and C. Altona, *Pseurot 6.2, A Program for the Conformational Analysis of Five Membered Rings*; University of Leiden, Leiden, The Netherlands, 1995.

44 K. Bondensgaard, M. Petersen, S. K. Singh, V. K. Rajwanshi, J. Wengel and J. P. Jacobsen, *Chem. Eur. J.*, 2000, **6**, 2687.
45 H. Liu, H. P. Spielmann, N. A. Ulyanov, D. E. Wemmer and T. L. James, *J. Biomol. NMR*, 1995, **6**, 390.
46 B. A. Borgias and T. L. James, *J. Magn. Reson.*, 1990, **87**, 475.
47 D. A. Case, D. A. Pearlman, J. W. Caldwell, T. E. Cheatham III, W. S. Ross, C. L. Simmerling, T. A. Darden, K. M. Merz, R. V. Stanton, A. L. Cheng, J. J. Vincent, M. Crowley, D. M. Ferguson, R. J. Radmer, G. L. Seibel, U. C. Singh, P. K. Weiner and P. A. Kollman, *AMBER 5*, University of California, San Francisco, 1997.
48 C. I. Bayly, P. Cieplak, W. D. Cornell and P. A. Kollman, *J. Phys. Chem.*, 1993, **97**, 10269.